Region Control of a Family of C-1 Rational Trigonometric Interpolation Spline Surfaces

Yixin Liu and Yuanpeng Zhu

***Abstract*—A family of C^1 rational cubic/linear trigonometric interpolation splines are utilized to generate blending interpolation surfaces. The data-based sufficient conditions concerning the local control factors are deduced to discuss the region control. These conditions guarantee that the surfaces strictly lie within two specified piecewise quadratic trigonometric blending interpolation surfaces. Additionally, some numerical experiments are conducted to demonstrate the region control of the surface under the proposed conditions.**

***Index Terms*—trigonometric splines, interpolation surface, region control, C^1 continuity.**

I. Introduction

FOR the construction of interpolation curves and surfaces using given data, several key factors should be taken into account. Computational efficiency is paramount, as it determines how quickly and effectively we can generate the desired surfaces. Smoothness is also crucial, as it ensures that the resulting surfaces are visually appealing and physically meaningful. Additionally, the capability to preserve the shape characteristics is essential to maintaining the integrity of the interpolated surfaces. Given that cubic functions strike a balance between accuracy and efficiency, and C^1 continuity is sufficient for majority of applications, the primary objective of this work is to study interpolation splines and their surfaces, with a particular emphasis on region control.

There exist lots of C^1 interpolation curves generated by rational cubic splines with different denominators. For example, Hussain and Sarfraz [1] constructed interpolation curves using rational cubic/quadratic interpolation splines. They further studied the positivity-preserving property but the associated constraints are insufficient. Qin et al. [2] later addressed this limitation by adding a local parameter with tension property. Additionally, based on Gregory's rational cubic splines [3], a region-restricted interpolation method is proposed [4]. Using linear denominator, the constrained interpolation are further studied [5]. However, there are still instances where this interpolation cannot be solved, indicating the absence of positive parameters that ensure the region control. To enhance the constraining ability, Duan et al. [6]–[8] further developed some rational cubic interpolation splines with linear or quadratic denominators by incorporating weights. However, the conditions for the region control are non-explicit, making them impractical for applications.

Manuscript received December 11, 2024; revised April 29, 2025. The research was funded by the Natural Science Foundation Guangdong Province, China (Nos. 2024A1515010413, 2025A1515011263).

Yixin Liu is a postgraduate student at School of Mathematics, South China University of Technology, Guangzhou, 510641, China. (e-mail: 202320129608@mail.scut.edu.cn).

Yuanpeng Zhu is a professor at School of Mathematics, South China University of Technology, Guangzhou, 510641, China. (corresponding author to provide e-mail: ypzhu@scut.edu.cn).

To further expand the range of applications, several C^1 rational cubic interpolation splines have been studied on two-dimensional case. Using a Hermite-like basis, Hussain and Sarfraz [1] introduced rational bi-cubic functions along with conditions of the local control parameters. However, this method required cross-boundary derivatives or twists. In response to this, by means of the Boolean sum, Hussain et al. [9] proposed a simple scheme to blend rational cubic splines that serve as bounds. However, Abbas et al. [10] pointed out that this method does not guarantee monotonicity or positivity of the entire surfaces and only preserve the shape characteristics at the boundary. The question arose as to whether it is feasible to create interpolation surfaces that preserve monotonicity or positivity by constraining the bounds of each local patch. Following this, a type of C^1 bi-cubic blending interpolation splines with linear denominators was proposed [11]. The new sufficient constraints on the bounds for the positivity or monotonicity-preservation of surfaces are given. Chan and Ong [12] proposed a range-restricted local construction method for C^1 interpolating curved surfaces, using constant to cubic polynomial surfaces as bounds. Brodlie et al. [13] proposed a modified quadratic Shepard method that restricts the interpolation values to the range $[0, 1]$ and can be extended to the case with arbitrary boundary functions. Qin and Xu [14] proposed a type of C^1 rational cubic trigonometric (RCT) interpolation spline with linear denominators. Their work has focused primarily on the positivity-preserving property, an essential aspect that ensures the non-negativity of the interpolated surfaces. However, in the realm of scientific and engineering applications, the precise control of surface geometry extends beyond mere positivity preservation. Region control plays an important role in ensuring that the resulting surfaces adhere strictly to desired geometric constraints. Therefore, our study aims to delve deeper into the region control property by doing the following important work:

(1) We deduced the simple and explicit conditions to guarantee that the resulting surface strictly lies within two specific piecewise quadratic trigonometric blending interpolation surfaces.

(2) We used four 3D data sets in the numerical examples, showing that our method ensures that RCT interpolation surface satisfies specific geometric constraints within designated regions, which enables practitioners to create surfaces that meet functional requirements and strictly adhere to geometric constraints.

II. C^1 RCT interpolation splines and blending surfaces

A. C^1 RCT interpolation splines

Given monotonically increasing knots $\{u_i\}_{i=1}^n \subset R$ with the corresponding data set $\{p_i\}_{i=1}^n \subset R$. For $u \in [u_i, u_{i+1}]$, the piecewise RCT interpolation spline constructed by Qin and Xu [14] is

$$R(u) = B_0(x;\alpha_i)p_i + B_1(x;\alpha_i)\left[p_i + \frac{2h_i}{\pi(1+\alpha_i)}d_i\right] + B_2(x;\beta_i)\left[p_{i+1} - \frac{2h_i}{\pi(1+\beta_i)}d_{i+1}\right] + B_3(x;\beta_i)p_{i+1}, \tag{1}$$

where $x = \pi(u-u_i)/(2h_i)$, $h_i = u_{i+1}-u_i > 0$, α_i and β_i are non-negative local factors, and $d_i \in R$ serves as the first derivative at u_i. The RCT basis functions are defined as

$$\begin{cases} B_0(x;\alpha_i) = \dfrac{1-\sin x}{1+\alpha_i \sin x}, \\ B_1(x;\alpha_i) = \dfrac{\sin x(1-\sin x)(1+\alpha_i+\alpha_i\sin x)}{1+\alpha_i\sin x}, \\ B_2(x;\beta_i) = \dfrac{\cos x(1-\cos x)(1+\beta_i+\beta_i\cos x)}{1+\beta_i\cos x}, \\ B_3(x;\beta_i) = \dfrac{1-\cos x}{1+\beta_i\cos x}. \end{cases} \tag{2}$$

For practical applications, the first derivative d_i is often unknown and need to be predetermined. We determine them by the arithmetic mean method as

$$\begin{cases} d_1 = \Delta_1 - \dfrac{h_1}{h_1+h_2}\left(\Delta_2 - \Delta_1\right), \\ d_k = \dfrac{\Delta_{k-1}+\Delta_k}{2}, \quad k = 2,3,...,n-1, \\ d_n = \Delta_{n-1} + \dfrac{h_{n-1}}{h_{n-2}+h_{n-1}}\left(\Delta_{n-1}-\Delta_{n-2}\right), \end{cases}$$

where $\Delta_k = (p_{k+1}-p_k)/h_k$. This arithmetic mean method, using three-point difference approximation grounded in arithmetic calculation, is computationally efficient and suitable for visualization of shaped data. And it has been used in many works [15], [16].

To clarify the relationship between the piecewise spline $R(u)$ on $[u_i, u_{i+1}]$ and the associated factors, we also adopt the notation $R(u; p_i, p_{i+1}; d_i, d_{i+1}; \alpha_i, \beta_i)$ for further discussions.

B. C^1 blending RCT interpolation surfaces

Given a domain $\Omega = [a,b]\times[c,d]$ with two associated partition $a = u_1 < u_2 < ... < u_n = b$, $c = v_1 < v_2 < \ldots < v_m = d$, and corresponding data (u_i, v_j, P_{ij}). Based on the RCT interpolation splines stated in (1), four boundary functions for patch $\pi_{i,j} := [u_i, u_{i+1}]\times[v_j, v_{j+1}]$ can be constructed. These bounds are then blended by the Boolean sum of quadratic trigonometric interpolation operators [14], resulting in a blending RCT interpolation surface as

$$\begin{aligned} S(u,v) &:= \left(\left(Q_1 \oplus Q_2\right)P\right)(u,v) \\ &= \left(Q_1P\right)(u,v) + \left(Q_2P\right)(u,v) - \left(Q_1Q_2P\right)(u,v), \end{aligned} \tag{3}$$

where

$$\begin{cases} \left(Q_1P\right)(u,v) := \begin{bmatrix} P(u_i,v) & P(u_{i+1},v) \end{bmatrix} \begin{bmatrix} b_0(x) \\ b_1(x) \end{bmatrix}, \\ \left(Q_2P\right)(u,v) := \begin{bmatrix} P(u,v_j) & P(u,v_{j+1}) \end{bmatrix} \begin{bmatrix} b_0(y) \\ b_1(y) \end{bmatrix}, \\ \left(Q_1Q_2P\right)(u,v) \\ := \begin{bmatrix} b_0(x) & b_1(x) \end{bmatrix} \begin{bmatrix} P_{i,j} & P_{i,j+1} \\ P_{i+1,j} & P_{i+1,j+1} \end{bmatrix} \begin{bmatrix} b_0(y) \\ b_1(y) \end{bmatrix}, \end{cases} \tag{4}$$

with $x = \pi(u-u_i)/(2h_i^u)$, $y = \pi(v-v_j)/(2h_j^v)$, $h_i^u = u_{i+1}-u_i$, $h_j^v = v_{j+1}-v_j$, and

$$\begin{cases} b_0(x) := \cos^2 x, \; b_1(x) := \sin^2 x, \\ b_0(y) := \cos^2 y, \; b_1(y) := \sin^2 y, \\ P(u,v_j) := R(x; P_{i,j}, P_{i+1,j}; D^u_{i,j}, D^u_{i+1,j}; \alpha^u_{i,j}, \beta^u_{i,j}), \\ P(u_i,v) := R(y; P_{i,j}, P_{i,j+1}; D^v_{i,j}, D^v_{i,j+1}; \alpha^v_{i,j}, \beta^v_{i,j}). \end{cases} \tag{5}$$

$\alpha^u_{i,j}$, $\beta^u_{i,j}$, $\alpha^v_{i,j}$, $\beta^v_{i,j}$ serve as local factors and $D^u_{i,j}$, $D^v_{i,j}$ serve as the first partial derivatives at (u_i, v_i) . According to the formula of $S(u,v)$ stated in (4), the modification of any one local factor $\alpha^u_{i,j}$, $\alpha^v_{i,j}$, $\beta^u_{i,j}$ or $\beta^v_{i,j}$ will only affect the shape on the corresponding patch $\pi_{i,j}$. From the C^1 continuity of the bounds and blending functions given in (5), it is obvious that the blending RCT surface $S(u,v)$ is global C^1 continuous.

Next, we determine the first partial derivatives by the arithmetic mean method again,

$$\begin{cases} D^u_{1,l} = \Delta^u_{1,l} + (\Delta^u_{1,l} - \Delta^u_{2,l})\dfrac{h^u_1}{h^u_1+h^u_2}, \\ D^u_{k,l} = \dfrac{\Delta^u_{k-1,l}+\Delta^u_{k,l}}{2}, \; k = 2,3,...,n-1, \\ \qquad l = 1,2,...,m, \\ D^u_{n,l} = \Delta^u_{n-1,l} + (\Delta^u_{n-1,l} - \Delta^u_{n-2,l})\dfrac{h^u_{n-1}}{h^u_{n-2}+h^u_{n-1}}, \\ D^v_{k,1} = \Delta^v_{k,1} + (\Delta^v_{k,1} - \Delta^v_{k,2})\dfrac{h^v_1}{h^v_1+h^v_2}, \\ D^v_{k,l} = \dfrac{\Delta^v_{k,l-1}+\Delta^v_{k,l}}{2}, \; k = 1,2,...,n, \\ \qquad l = 2,3,...,m-1, \\ D^v_{k,m} = \Delta^v_{k,m-1} + (\Delta^v_{k,m-1} - \Delta^v_{k,m-2})\dfrac{h^v_{m-1}}{h^v_{m-2}+h^v_{m-1}}, \end{cases} \tag{6}$$

where $\Delta^u_{k,l} = (P_{k+1,l} - P_{k,l})/h^u_k$ and $\Delta^v_{k,l} = (P_{k,l+1} - P_{k,l})/h^v_l$.

III. The RCT interpolation surfaces with region control

The aim of this section is to establish an explicit scheme that ensures the blending RCT interpolation surface $S(u,v)$ mentioned in (3) strictly lies within two specific quadratic trigonometric blending interpolation surfaces.

Given data sets $\{(u_i, v_j, H_{i,j})\}$, $\{(u_i, v_j, H^*_{i,j})\}$ and $\{(u_i, v_j, P_{i,j})\}$ defined on the domain Ω and satisfying $H_{i,j} \le P_{i,j} \le H^*_{i,j}$. For simplicity, we use the notation $T_{i,j} := P_{i,j} - H_{i,j}$, $T^*_{i,j} := P_{i,j} - H^*_{i,j}$ for further discussion. $S(u,v)$ denotes the blending RCT interpolation surface generated by $\{(u_i, v_j, P_{i,j})\}$, $H(u,v)$ and $H^*(u,v)$

denote the quadratic trigonometric blending interpolation surfaces generated by $\{(u_i, v_j, H_{i,j})\}$ and $\{(u_i, v_j, H^*_{i,j})\}$, respectively, as

$$\begin{aligned}&H(u,v) := ((Q_1 \oplus Q_2) H)(u,v)\\&= (Q_1H)(u,v) + (Q_2H)(u,v) - (Q_1Q_2H)(u,v),\\&H^*(u,v) := ((Q_1 \oplus Q_2) H^*)(u,v)\\&= (Q_1H^*)(u,v) + (Q_2H^*)(u,v) - (Q_1Q_2H^*)(u,v),\end{aligned} \tag{7}$$

where

$$\begin{cases}(Q_1H)(u,v) := \begin{bmatrix} H(u_i,v) & H(u_{i+1},v)\end{bmatrix}\begin{bmatrix} b_0(x)\\ b_1(x)\end{bmatrix},\\(Q_2H)(u,v) := \begin{bmatrix} H(u,v_j) & H(u,v_{j+1})\end{bmatrix}\begin{bmatrix} b_0(y)\\ b_1(y)\end{bmatrix},\\(Q_1Q_2H)(u,v)\\:= \begin{bmatrix} b_0(x) & b_1(x)\end{bmatrix}\begin{bmatrix} H_{i,j} & H_{i,j+1}\\ H_{i+1,j} & H_{i+1,j+1}\end{bmatrix}\begin{bmatrix} b_0(y)\\ b_1(y)\end{bmatrix},\\(Q_1H^*)(u,v) := \begin{bmatrix} H^*(u_i,v) & H^*(u_{i+1},v)\end{bmatrix}\begin{bmatrix} b_0(x)\\ b_1(x)\end{bmatrix},\\(Q_2H^*)(u,v) := \begin{bmatrix} H^*(u,v_j) & H^*(u,v_{j+1})\end{bmatrix}\begin{bmatrix} b_0(y)\\ b_1(y)\end{bmatrix},\\(Q_1Q_2H^*)(u,v)\\:= \begin{bmatrix} b_0(x) & b_1(x)\end{bmatrix}\begin{bmatrix} H^*_{i,j} & H^*_{i,j+1}\\ H^*_{i+1,j} & H^*_{i+1,j+1}\end{bmatrix}\begin{bmatrix} b_0(y)\\ b_1(y)\end{bmatrix},\end{cases}$$

with $x = \pi(u-u_i)/(2h^u_i)$, $y = \pi(v-v_j)/(2h^v_j)$, $h^u_i = u_{i+1} - u_i$, $h^v_j = v_{j+1} - v_j$, and

$$\begin{cases}H(u,v_j) := \cos^2(x)H_{i,j} + \sin^2(x)H_{i+1,j},\\H(u,v_{j+1}) := \cos^2(x)H_{i,j+1} + \sin^2(x)H_{i+1,j+1},\\H(u_i,v) := \cos^2(y)H_{i,j} + \sin^2(y)H_{i,j+1},\\H(u_{i+1},v) := \cos^2(y)H_{i+1,j} + \sin^2(y)H_{i+1,j+1},\\H^*(u,v_j) := \cos^2(x)H^*_{i,j} + \sin^2(x)H^*_{i+1,j},\\H^*(u,v_{j+1}) := \cos^2(x)H^*_{i,j+1} + \sin^2(x)H^*_{i+1,j+1},\\H^*(u_i,v) := \cos^2(y)H^*_{i,j} + \sin^2(y)H^*_{i,j+1},\\H^*(u_{i+1},v) := \cos^2(y)H^*_{i+1,j} + \sin^2(y)H^*_{i+1,j+1}.\end{cases}$$

Now, we proceed to deduce sufficient conditions for the region control. To this end, we analyze the case where $S(u,v)$ strictly lies above $H(u,v)$. Without loss of generality, we confine our discussion to a local patch $\pi_{i,j}$, and obtain

$$\begin{aligned}&S(u,v) - H(u,v)\\=&b_0(x)\left[P(u_i,v) - H(u_i,v)\right] + b_1(x)\left[P(u_{i+1},v)\right.\\&\left.- H(u_{i+1},v)\right] + b_0(y)\left[P(u,v_j) - H(u,v_j)\right]\\&+ b_1(y)\left[P(u,v_{j+1}) - H(u,v_{j+1})\right] - b_0(x)b_0(y)T_{i,j}\\&- b_0(x)b_1(y)T_{i,j+1} - b_1(x)b_0(y)T_{i+1,j}\\&- b_1(x)b_1(y)T_{i+1,j+1}\\=&b_0(x)\left[P(u,v_j) - H(u,v_j) - \frac{1}{2}b_0(x)T_{i,j}\right.\\&\left.-\frac{1}{2}b_1(y)T_{i+1,j}\right] + b_1(x)\left[P(u,v_{j+1}) - H(u,v_{j+1})\right.\\&\left.-\frac{1}{2}b_0(x)T_{i,j+1} - \frac{1}{2}b_1(y)T_{i+1,j+1}\right] + b_0(y)\left[P(u_i,v)\right.\\&\left.-H(u_i,v) - \frac{1}{2}b_0(x)T_{i,j} - \frac{1}{2}b_1(y)T_{i,j+1}\right]\\&+ b_1(y)\left[P(u_{i+1},v) - H(u_{i+1},v) - \frac{1}{2}b_0(x)T_{i+1,j}\right.\\&\left.-\frac{1}{2}b_1(y)T_{i+1,j+1}\right].\end{aligned}$$

From the positivity of $b_0(\zeta)$ and $b_1(\zeta)$ for any $\zeta \in (0,1)$, we can infer that $S(u,v) > H(u,v)$ for $(u,v) \in \pi_{i,j}$, if

$$\begin{cases}P(u,v_j) - H(u,v_j) - \frac{1}{2}b_0(x)T_{i,j} - \frac{1}{2}b_1(y)T_{i+1,j} > 0,\\P(u,v_{j+1}) - H(u,v_{j+1}) - \frac{1}{2}b_0(x)T_{i,j+1}\\\qquad -\frac{1}{2}b_1(y)T_{i+1,j+1} > 0,\\P(u_i,v) - H(u_i,v) - \frac{1}{2}b_0(x)T_{i,j} - \frac{1}{2}b_1(y)T_{i,j+1} > 0,\\P(u_{i+1},v) - H(u_{i+1},v) - \frac{1}{2}b_0(x)T_{i+1,j}\\\qquad -\frac{1}{2}b_1(y)T_{i+1,j+1} > 0.\end{cases} \tag{8}$$

By simple computations, we have

$$\begin{aligned}&P(u,v_j) - H(u,v_j) - \frac{1}{2}b_0(x)T_{i,j} - \frac{1}{2}b_1(x)T_{i+1,j}\\=&\frac{1}{2}B_0(x;\alpha^u_{i,j})T_{i,j} + B_1(x;\alpha^u_{i,j})\left[\frac{T_{i,j}}{2} + \frac{2h_iD^u_{i,j}}{\pi(1+\alpha^u_{i,j})}\right]\\&+ B_2(x;\beta^u_{i,j})\left[\frac{T_{i+1,j}}{2} - \frac{2h_iD^u_{i+1,j}}{\pi(1+\beta^u_{i,j})}\right]\\&+ \frac{1}{2}B_3(x;\beta^u_{i,j})T_{i+1,j}.\end{aligned} \tag{9}$$

It is clear that (9) will be positive if the four coefficients are non-negative, from which we get the following sufficient conditions,

$$\begin{cases}\alpha^u_{i,j} \geq \max\left\{0, -1 - \frac{4h_iD^u_{i,j}}{\pi T_{i,j}}\right\},\\\beta^u_{i,j} \geq \max\left\{0, -1 + \frac{4h_iD^u_{i+1,j}}{\pi T_{i+1,j}}\right\}.\end{cases}$$

The sufficient conditions for the remaining three inequalities in (8) can be obtained in a similar way, which subsequently lead to the sufficient conditions for $S(u,v) > H(u,v)$ when $(u,v) \in \Omega$, as outlined below,

$$\begin{cases}\alpha^u_{i,j} \geq \max\left\{0, -1 - \frac{4h_iD^u_{i,j}}{\pi T_{i,j}}\right\},\\\beta^u_{i,j} \geq \max\left\{0, -1 + \frac{4h_iD^u_{i+1,j}}{\pi T_{i+1,j}}\right\},\\\alpha^v_{i,j} \geq \max\left\{0, -1 - \frac{4h_iD^v_{i,j}}{\pi T_{i,j}}\right\},\\\beta^v_{i,j} \geq \max\left\{0, -1 + \frac{4h_iD^v_{i,j+1}}{\pi T_{i,j+1}}\right\}.\end{cases} \tag{10}$$

Then, we consider $S(u,v)$ strictly lies below $H^*(u,v)$. Similarly, we have

$$\begin{aligned}&H^*(u,v) - S(u,v)\\=&b_0(x)\left[H^*(u_i,v) - P(u_i,v)\right] + b_1(x)\left[H^*(u_{i+1},v)\right.\\&\left.-P(u_{i+1},v)\right] + b_0(y)\left[H^*(u,v_j) - P(u,v_j)\right]\end{aligned}$$

$$
\begin{aligned}
&+ b_1(y)\left[H^*(u,v_{j+1}) - P(u,v_{j+1})\right] + b_0(x)b_0(y)T^*_{i,j}+ \\
&b_0(x)b_1(y)T^*_{i,j+1} + b_1(x)b_0(y)T^*_{i+1,j} \\
&+ b_1(x)b_1(y)T^*_{i+1,j+1} \\
=&b_0(y)\left[H^*(u,v_j) - P(u,v_j) + \frac{1}{2}b_0(x)T^*_{i,j}\right. \\
&\left.+\frac{1}{2}b_1(x)T^*_{i+1,j}\right] + b_1(y)\left[H^*(u,v_{j+1}) - P(u,v_{j+1})\right. \\
&\left.+\frac{1}{2}b_0(x)T^*_{i,j+1} + \frac{1}{2}b_1(x)T^*_{i+1,j+1}\right] \\
&+ b_0(x)\left[H^*(u_i,v) - P(u_i,v) + \frac{1}{2}b_0(y)T^*_{i,j}\right. \\
&\left.+\frac{1}{2}b_1(y)T^*_{i,j+1}\right] + b_1(x)\left[H^*(u_{i+1},v)\right. \\
&\left.-P(u_{i+1},v) + \frac{1}{2}b_0(y)T^*_{i+1,j} + \frac{1}{2}b_1(y)T^*_{i+1,j+1}\right].
\end{aligned}
$$

From these, we can infer that $H^*(u,v) > S(u,v)$ in the patch $\pi_{i,j}$, if

$$
\begin{cases}
H^*(u,v_j) - P(u,v_j) + \frac{1}{2}b_0(x)T^*_{i,j} + \frac{1}{2}b_1(x)T^*_{i+1,j} > 0, \\
H^*(u,v_{j+1}) - P(u,v_{j+1}) + \frac{1}{2}b_0(x)T^*_{i,j+1} \\
\qquad\qquad + \frac{1}{2}b_1(x)T^*_{i+1,j+1} > 0, \\
H^*(u_i,v) - P(u_i,v) + \frac{1}{2}b_0(y)T^*_{i,j} + \frac{1}{2}b_1(y)T^*_{i,j+1} > 0, \\
H^*(u_{i+1},v) - P(u_{i+1},v) + \frac{1}{2}b_0(y)T^*_{i+1,j} \\
\qquad\qquad + \frac{1}{2}b_1(y)T^*_{i+1,j+1} > 0.
\end{cases}
\tag{11}
$$

By simple computations, we have

$$
\begin{aligned}
&G^*(u,v_j) - H(u,v_j) - \frac{1}{2}b_0(t)\left(H^*_{i,j} - P_{i,j}\right) \\
&\quad -\frac{1}{2}b_1(t)\left(H^*_{i+1,j} - P_{i+1,j}\right) \\
&= -\frac{1}{2}B_0(x;\alpha^u_{i,j})T^*_{i,j} - B_1(x;\alpha^u_{i,j})\left[\frac{T^*_{i,j}}{2} + \frac{2h_iD^u_{i,j}}{\pi(1+\alpha^u_{i,j})}\right] \\
&\quad -B_2(x;\beta^u_{i,j})\left[\frac{T^*_{i+1,j}}{2} - \frac{2h_iD^u_{i+1,j}}{\pi(1+\beta^u_{i,j})}\right] \\
&\quad -\frac{1}{2}B_3(x;\beta^u_{i,j})T^*_{i+1,j+1}.
\end{aligned}
\tag{12}
$$

It is easy to check that (12) will be positive if

$$
\begin{cases}
\alpha^u_{i,j} \geq \max\left\{0, -1 - \dfrac{4h_iD^u_{i,j}}{\pi T^*_{i,j}}\right\}, \\
\beta^u_{i,j} \geq \max\left\{0, -1 + \dfrac{4h_iD^u_{i+1,j}}{\pi T^*_{i+1,j}}\right\}.
\end{cases}
$$

Then we derive the sufficient conditions for the remaining three inequalities in (11), which subsequently lead to the sufficient conditions for $H^*(u,v) > S(u,v)$ when $(u,v) \in \Omega$, as outlined below,

$$
\begin{cases}
\alpha^u_{i,j} \geq \max\left\{0, -1 - \dfrac{4h_iD^u_{i,j}}{\pi T^*_{i,j}}\right\}, \\
\beta^u_{i,j} \geq \max\left\{0, -1 + \dfrac{4h_iD^u_{i+1,j}}{\pi T^*_{i+1,j}}\right\}, \\
\alpha^v_{i,j} \geq \max\left\{0, -1 - \dfrac{4h_iD^v_{i,j}}{\pi T^*_{i,j}}\right\}, \\
\beta^v_{i,j} \geq \max\left\{0, -1 + \dfrac{4h_iD^v_{i,j+1}}{\pi T^*_{i,j+1}}\right\}.
\end{cases}
\tag{13}
$$

Now, combining (10) with (13), sufficient conditions for the region control on the entire domain Ω can be summarized as the following theorem,

Theorem III.1. *Given data sets $\{(u_i,v_j,H_{i,j})\}$, $\{(u_i,v_j,H^*_{i,j})\}$ and $\{(u_i,v_j,P_{i,j})\}$ defined on the domain Ω and satisfying $H_{i,j} \leq P_{i,j} \leq H^*_{i,j}$. $S(u,v)$ is the resulting RCT surface given in* (3)*, $H(u,v)$ and $H^*(u,v)$ are the resulting quadratic trigonometric blending surfaces given in* (7)*. If all the local control factors in the RCT surface satisfy*

$$
\begin{cases}
\alpha^u_{i,j} = \max\left\{0, -1 - \dfrac{4h_iD^u_{i,j}}{\pi T_{i,j}}, -1 - \dfrac{4h_iD^u_{i,j}}{\pi T^*_{i,j}}\right\} + \rho^u_{i,j}, \\
\beta^u_{i,j} = \max\left\{0, 1 + \dfrac{4h_iD^u_{i+1,j}}{\pi T_{i+1,j}}, -1 + \dfrac{4h_iD^u_{i+1,j}}{\pi T^*_{i+1,j}}\right\} \\
\qquad\qquad\qquad\qquad\qquad\qquad +\sigma^u_{i,j}, \\
\alpha^v_{i,j} = \max\left\{0, -1 - \dfrac{4h_iD^v_{i,j}}{\pi T_{i,j}}, -1 - \dfrac{4h_iD^v_{i,j}}{\pi T^*_{i,j}}\right\} + \rho^v_{i,j}, \\
\beta^v_{i,j} = \max\left\{0, -1 + \dfrac{4h_iD^v_{i,j+1}}{\pi T_{i,j+1}}, -1 + \dfrac{4h_iD^v_{i,j+1}}{\pi T^*_{i,j+1}}\right\} \\
\qquad\qquad\qquad\qquad\qquad\qquad +\sigma^v_{i,j},
\end{cases}
\tag{14}
$$

where $\rho^u_{i,j}, \rho^v_{i,j}, \sigma^u_{i,j}, \sigma^v_{i,j}$ are non-negative parameters. Then, we have $H(u,v) < S(u,v) < H^*(u,v)$.

IV. Numerical experiments

In this section, we conduct some numerical experiments to exam the region control concerning the C^1 RCT interpolation surface under the proposed conditions (14). In Figure 1, the data $\{(u_i,v_j,P_{i,j})\}$ are presented in Table I with $H^*_{i,j} = P_{i,j} + 0.14$, $H_{i,j} = P_{i,j} - 0.14$. Figure 1(a) demonstrates the interpolation surface $S_1(u,v)$ constructed by setting all parameters $\rho^u_{i,j} = \rho^v_{i,j} = \sigma^u_{i,j} = \sigma^v_{i,j} = 0$. Figure 1(d) demonstrates the interpolation surface $S_2(u,v)$ constructed by setting all parameters $\rho^u_{i,j} = \rho^v_{i,j} = \sigma^u_{i,j} = \sigma^v_{i,j} = 1.2$.

In Figure 2, the data $\{(u_i,v_j,P_{i,j})\}$ are presented in Table II with $H^*_{i,j} = P_{i,j}+0.2$, $H_{i,j} = P_{i,j}-0.2$. Figure 2(a) demonstrates the interpolation surface $S_1(u,v)$ constructed by setting all parameters $\rho^u_{i,j} = \rho^v_{i,j} = \sigma^u_{i,j} = \sigma^v_{i,j} = 0$. Figure 2(d) demonstrates the interpolation surface $S_2(u,v)$ constructed by setting all parameters $\rho^u_{i,j} = \rho^v_{i,j} = \sigma^u_{i,j} = \sigma^v_{i,j} = 1.2$.

In Figure 3, the data $\{(u_i,v_j,P_{i,j})\}$ are presented in Table III with $H^*_{i,j} = P_{i,j}+0.8$, $H_{i,j} = P_{i,j}-0.8$. Figure 3(a) demonstrates the interpolation surface $S_1(u,v)$ constructed by setting all parameters $\rho^u_{i,j} = \rho^v_{i,j} = \sigma^u_{i,j} = \sigma^v_{i,j} = 0$.

TABLE I: The 3D data set given by Hussain and Sarfraz [1].

y/x	-3	-2	-1	1	2	3
-3	0.0124	0.0238	0.0404	0.0404	0.0238	0.0124
-2	0.0238	0.0635	0.1667	0.1667	0.0635	0.0238
-1	0.0404	0.1667	1.3333	1.3333	0.1667	0.0404
1	0.0404	0.1667	1.333	1.3333	0.1667	0.0404
2	0.0238	0.0635	0.1667	0.1667	0.0635	0.0238
3	0.0124	0.0238	0.0404	0.0404	0.0238	0.0124

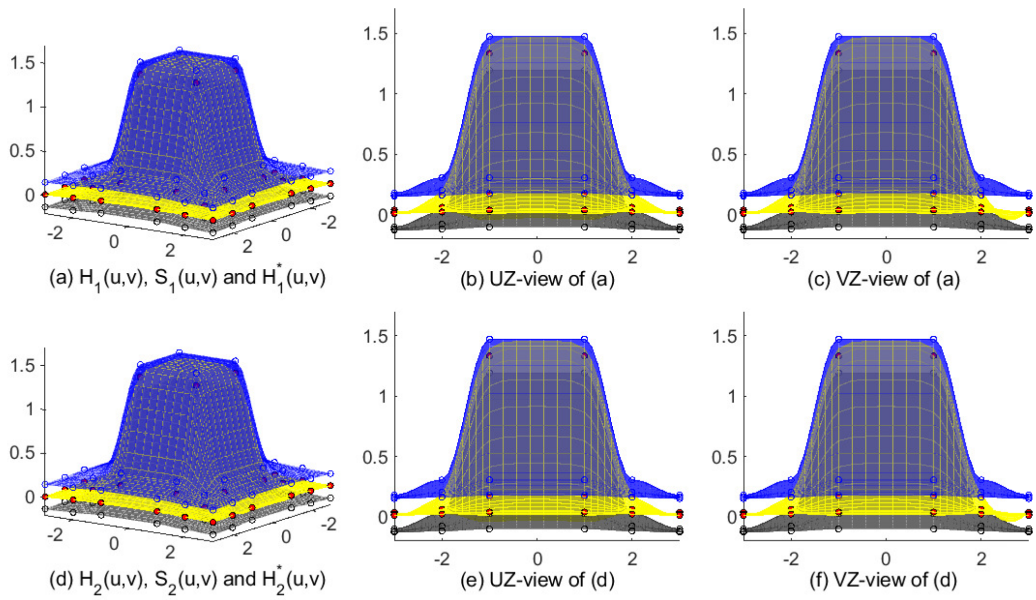

Fig. 1 The interpolation surface for the data stated in Table I.

TABLE II: The 3D data set given by Abbas et al. [10].

y/x	-3	-2	-1	0	1	2	3
-3	0.0401	0.0404	0.1755	1.0401	0.1755	0.0404	0.0401
-2	0.0583	0.0586	0.1936	1.0583	0.1936	0.0586	0.0583
-1	0.4078	0.4082	0.5432	1.4079	0.5432	0.4082	0.4078
0	1.0400	1.0403	1.1753	2.0400	1.1753	1.0403	1.0400
1	0.4078	0.4082	0.5432	1.4079	0.5432	0.4082	0.4078
2	0.0583	0.0586	0.1936	1.0583	0.1936	0.0586	0.0583
3	0.0401	0.0404	0.1755	1.0401	0.1755	0.0404	0.0401

Figure 3(d) demonstrates the interpolation surface $S_2(u,v)$ constructed by setting all parameters $\rho^u_{i,j} = \rho^v_{i,j} = \sigma^u_{i,j} = \sigma^v_{i,j} = 1.2$.

In Figure 4, the data $\{(u_i, v_j, P_{i,j})\}$ are presented in Table IV with $H^*_{i,j} = P_{i,j}+14$, $H_{i,j} = P_{i,j}-14$. Figure 4(a) demonstrates the interpolation surface $S_1(u,v)$ constructed by setting all parameters $\rho^u_{i,j} = \rho^v_{i,j} = \sigma^u_{i,j} = \sigma^v_{i,j} = 0$. Figure 4(d) demonstrates the interpolation surface $S_2(u,v)$ constructed by setting all parameters $\rho^u_{i,j} = \rho^v_{i,j} = \sigma^u_{i,j} = \sigma^v_{i,j} = 1.2$.

We conclude that under the conditions in (14), the generated surfaces will strictly lie within two specific piecewise blending quadratic trigonometric interpolation surfaces. Additionally, the local free control factors enable the local modification of surface shapes.

V. Conclusions

Based on the C^1 RCT splines, we have discussed the region control of the generated surfaces in detail and deduced the explicit and sufficient conditions. In scientific and engineering applications, precise control of surface geometry is crucial. Our method, as evidenced by numerical findings, ensures that RCT interpolation surface satisfies specific geometric constraints within designated regions, which provides practitioners with reliable tools for achieving this control and enables them to create surfaces that meet functional requirements and strictly adhere to geometric constraints.

References

[1] M. Z. Hussain and M. Sarfraz, "Positivity-preserving interpolation of positive data by rational cubics," *Journal of computational and applied mathematics*, vol. 218, no. 2, pp. 446–458, 2008.

[2] X. Qin, L. Qin, and Q. Xu, "C^1 positivity-preserving interpolation schemes with local free parameters," *IAENG International Journal of Computer Science*, vol. 43, no. 2, pp. 219–227, 2016.

[3] J. A. Gregory, "Shape preserving spline interpolation," *NASA. Langley Research Center Computational Geometry and Computer-Aided Design*, 1985.

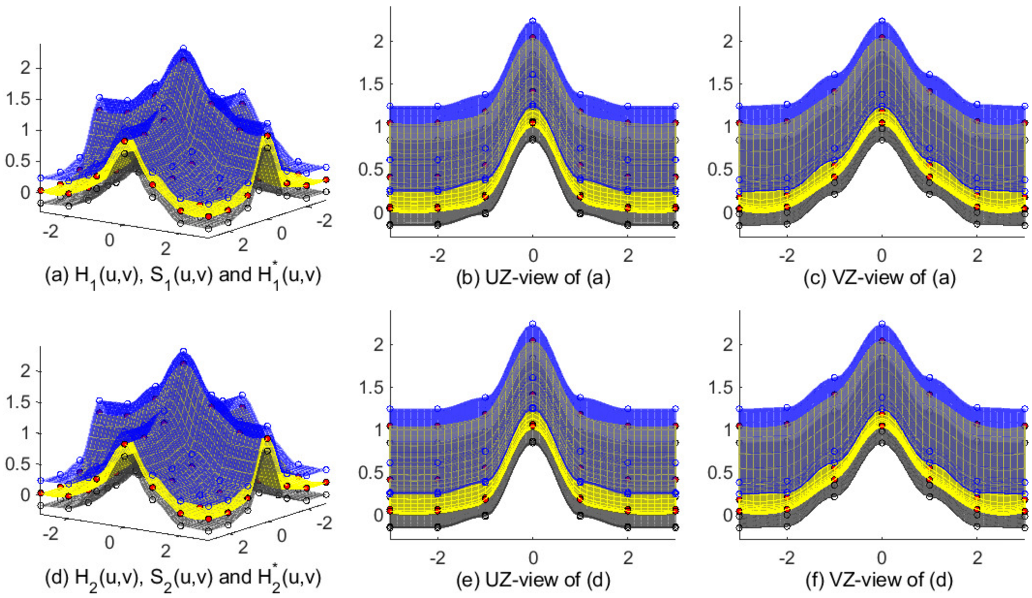

Fig. 2 The interpolation surface for the data stated in Table II.

TABLE III: The 3D data set given by Sarfraz et al. [15].

y/x	-3	-2	-1	1	2	3
-3	2.5000	4.8077	4.9000	0.1000	0.1923	2.5000
-2	0.1923	2.5000	3.7000	1.3000	2.5000	4.8077
-1	0.1000	1.3000	2.5000	2.5000	3.7000	4.9000
1	4.9000	3.7000	2.5000	2.5000	1.3000	0.1000
2	4.8077	2.5000	1.3000	3.7000	2.5000	0.1923
3	2.5000	0.1923	0.1000	4.9000	4.8077	2.5000

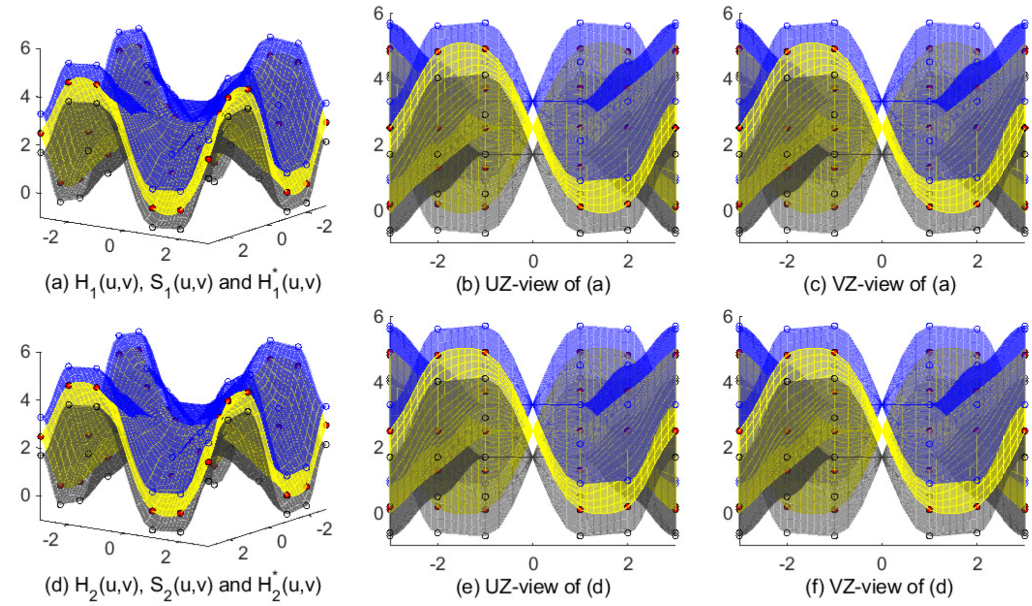

Fig. 3 The interpolation surface for the data stated in Table III.

[4] M. Bastian-Walther and J. W. Schmidt, “Range restricted interpolation using gregory’s rational cubic splines,” *Journal of computational and applied mathematics*, vol. 103, no. 2, pp. 221–237, 1999.

[5] Q. Duan, G. Xu, A. Liu, X. Wang, and F. Cheng, “Constrained interpolation using rational cubic spline with linear denominators,” *Korean Journal of Computational and Applied Mathematics*, vol. 6, pp. 203–215, 1999.

[6] Q. Duan, K. Djidjeli, W. Price, and E. Twizell, “Weighted rational cubic spline interpolation and its application,” *Journal of computational and applied mathematics*, vol. 117, no. 2, pp. 121–135, 2000.

[7] Q. Duan, L. Wang, and E. H. Twizell, “A new c^2 rational interpolation based on function values and constrained control of the interpolant curves,” *Applied Mathematics and Computation*, vol. 161, no. 1, pp. 311–322, 2005.

[8] Q. Duan, Y. Zhang, L. Wang, and E. Twizell, “Region control and approximation of a weighted rational interpolating curves,” *Communications in numerical methods in engineering*, vol. 22, no. 1, pp. 41–53, 2006.

[9] M. Z. Hussain, M. Hussain, and B. Aqeel, “Shape-preserving surfaces with constraints on tension parameters,” *Applied Mathematics and*

TABLE IV: The 3D data set given by Sarfraz et al. [15].

y/x	-3	-2	-1	0	1	2	3
-3	1	26	65	82	65	26	1
-2	26	1	10	17	10	1	26
-1	65	10	1	2	1	10	65
0	82	17	2	1	2	17	82
1	65	10	1	2	1	10	65
2	26	1	10	17	10	1	26
3	1	26	65	82	65	26	1

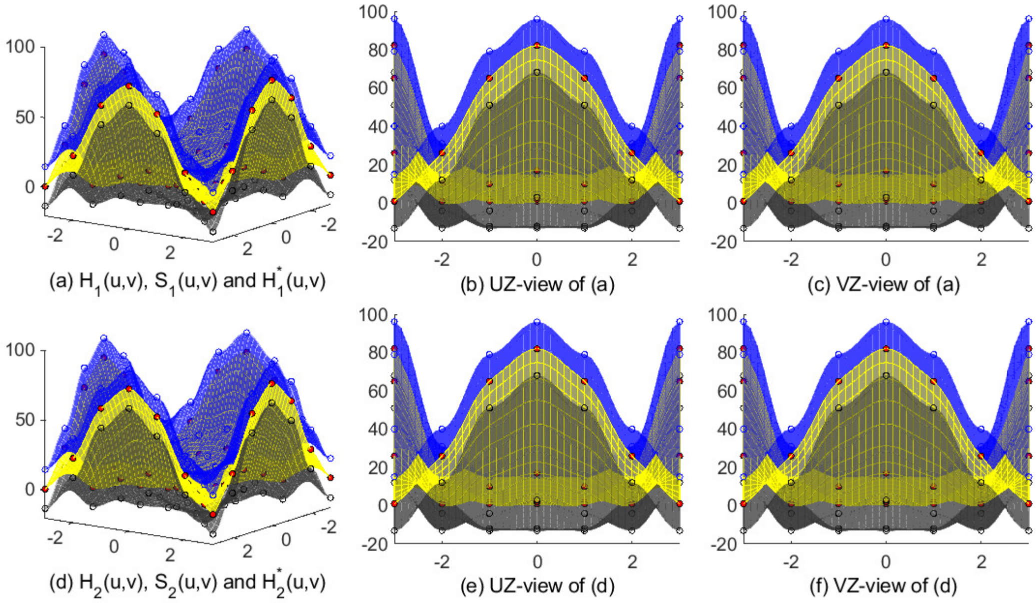

Fig. 4 The interpolation surface for the data stated in Table IV.

Computation, vol. 247, pp. 442–464, 2014.

[10] M. Abbas, A. A. Majid, and J. M. Ali, "Positivity-preserving rational bi-cubic spline interpolation for 3d positive data," *Applied Mathematics and Computation*, vol. 234, pp. 460–476, 2014.

[11] X. Qina, L. Qinb, and Q. Xua, "C^1 rational interpolation schemes for modelling positive and/or monotonic 3d data," *ScienceAsia*, vol. 43, no. 3, pp. 186–194, 2017.

[12] E. Chan and B. Ong, "Range restricted scattered data interpolation using convex combination of cubic bézier triangles," *Journal of Computational and Applied Mathematics*, vol. 136, no. 1-2, pp. 135–147, 2001.

[13] K. W. Brodlie, M. R. Asim, and K. Unsworth, "Constrained visualization using the shepard interpolation family," in *Computer Graphics Forum*, vol. 24, no. 4. Wiley Online Library, 2005, pp. 809–820.

[14] X. Qin and Q. Xu, "C^1 rational cubic/linear trigonometric interpolation spline with positivity-preserving property," *Engineering Letters*, vol. 25, no. 2, pp. 152–159, 2017.

[15] M. Sarfraz, M. Z. Hussain, and A. Nisar, "Positive data modeling using spline function," *Applied Mathematics and Computation*, vol. 216, no. 7, pp. 2036–2049, 2010.

[16] Y. Zhu and M. Wang, "A class of c^1 rational interpolation splines in one and two dimensions with region control," *Computational and Applied Mathematics*, vol. 39, no. 2, p. 69, 2020.